Neuron 51, 201–212, July 20, 2006 ©2006 Elsevier Inc. DOI 10.1016/j.neuron.2006.06.023

Coiled Coils Direct Assembly of a Cold-Activated TRP Channel

Pamela R. Tsuruda,[1] David Julius,[1] and Daniel L. Minor, Jr.[1,2,3,4,*]
[1] Department of Cellular and Molecular Pharmacology
[2] Cardiovascular Research Institute
[3] Department of Biochemistry and Biophysics
[4] California Institute for Quantitative Biomedical Research
University of California, San Francisco
San Francisco, California 94158

Summary

Transient receptor potential (TRP) channels mediate numerous sensory transduction processes and are thought to function as tetramers. TRP channel physiology is well studied; however, comparatively little is understood regarding TRP channel assembly. Here, we identify an autonomously folded assembly domain from the cold- and menthol-gated channel TRPM8. We show that the TRPM8 cytoplasmic C-terminal domain contains a coiled coil that is necessary for channel assembly and sufficient for tetramer formation. Cell biological experiments indicate that coiled-coil formation is required for proper channel maturation and trafficking and that the coiled-coil domain alone can act as a dominant-negative inhibitor of functional channel expression. Our data define an authentic TRP modular assembly domain, establish a clear role for coiled coils in ion channel assembly, demonstrate that coiled-coil assembly domains are a general feature of TRPM channels, and delineate a new tool that should be of general use in dissecting TRPM channel function.

Introduction

Transient receptor potential (TRP) channels comprise a large family of nonselective cation channels that contribute to a range of sensory processes, including thermosensation, phototransduction, chemosensation, and nociception (Clapham, 2003; Julius and Basbaum, 2001; Montell et al., 2002). In keeping with such varied physiological roles, TRP channels are activated by diverse stimuli that include exogenous chemical agonists (such as capsaicin and menthol), changes in ambient temperature, and neurotransmitters or growth factors that stimulate phospholipase C signaling systems (Clapham et al., 2003). A number of TRP channels respond to combinations of stimuli and function as polymodal signal detectors that assess changes in the chemical and physical environment of the cell. While the sphere of TRP channel function and physiology has received intensive study, little is presently known about TRP channel structure.

TRP channels are members of the cation channel superfamily that includes voltage-gated channels for calcium, potassium, and sodium, as well as cyclic nucleotide-gated channels (Hille, 2001). In common with other superfamily members, TRP channels are complexes consisting of four pore-forming subunits (Hoenderop et al., 2003; Kedei et al., 2001). Each subunit is thought to contain six transmembrane regions (S1–S6) in which the loop between transmembrane segments S5 and S6 constitutes the selectivity filter. The N- and C-terminal domains are thought to be intracellular, where they may engage in subunit-subunit interactions, associate with other cellular proteins, and interact with cytoplasmic factors.

Although TRP channels appear to share a common transmembrane scaffold, individual family members display varied mechanisms of activation and ion selectivity (Clapham et al., 2001). In accordance with these varied functions and physiological stimuli, TRP protein sequences are quite diverse and have identities that run as low as 20% across the different subfamilies (Clapham, 2003). This molecular variegation is particularly manifest within the cytoplasmic domains. Different TRP subtypes have intracellular ankyrin repeats, TRP domains, nudix hydrolase domains, and kinase domains (Clapham, 2003; Montell, 2005). Both the ankyrin repeats and TRP domains have been proposed to interact with components of the cytoskeleton or lipid bilayer (Howard and Bechstedt, 2004; Liedtke et al., 2000; Rohacs et al., 2005; Sotomayor et al., 2005), but the precise physiological roles for these elements remain enigmatic. Finally, some members of the TRPC, TRPM, and TRPV subfamilies have been suggested to contain cytoplasmic coiled-coil domains (Jenke et al., 2003; Montell, 2005).

Coiled coils are the most common and best understood protein-protein interaction domain (Lupas and Gruber, 2005; Woolfson, 2005). The hallmark structural feature is a heptad repeat, denoted $(abcdefg)_n$. Hydrophobic amino acids at the "a" and "d" positions form a nonpolar stripe along the helical surface that is used for multimerization (Crick, 1953). The identities of the "a" and "d" amino acids provide the dominant feature that determines whether a given coiled-coil helix will associate into a two-, three-, four-, or five-stranded bundle (Harbury et al., 1993, 1994; Malashkevich et al., 1996).

Several prior studies are suggestive of a role for TRP channel coiled coils in subunit-subunit interactions. Yeast two-hybrid experiments show that the putative N-terminal coiled-coil domain from *Drosophila* TRPγ is sufficient to mediate interactions with the N terminus of TRPL, a channel subunit with which TRPγ forms heteromeric channels in vivo (Xu et al., 2000). Other work has shown that deletions in TRPM4 and TRPV1 that eliminate predicted C-terminal coiled-coil domains impair the ability of these subunits to form homomeric interactions (Garcia-Sanz et al., 2004; Launay et al., 2004). While these observations are consistent with a role for these putative coiled-coil domains in assembly of functional TRP channels, direct evidence that any of these domains adopt a coiled-coil structure and form a quaternary complex is lacking (Garcia-Sanz et al., 2004). Thus, whether TRP channels have authentic coiled coils has remained a matter of conjecture.

*Correspondence: daniel.minor@ucsf.edu

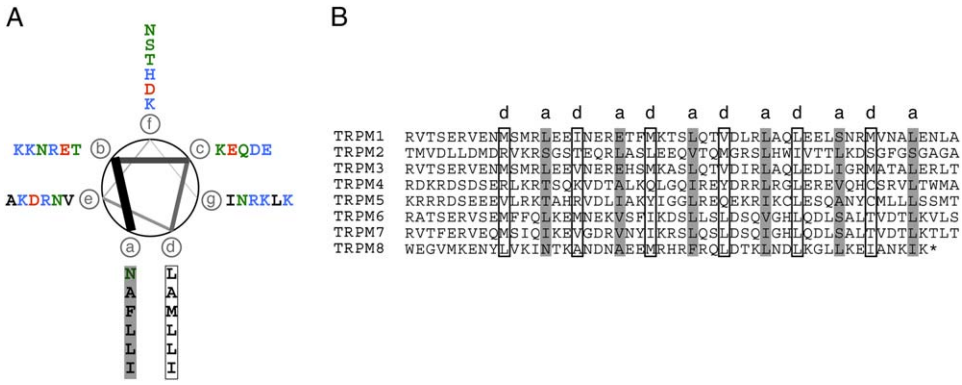

Figure 1. TRPM Coiled-Coil Domains

(A) Coiled-coil diagram of rat TRPM8 residues 1064–1104. Coiled-coil positions a–g are indicated. Amino acids are colored: hydrophobic, black; basic, blue; acidic, red; and polar, green.

(B) Alignment of conserved TRPM family coiled coils. "a" and "d" positions are indicated.

Recent studies of other ion channel families have shown that coiled-coil motifs contribute to mechanisms of subunit-subunit assembly (Jenke et al., 2003; Kanki et al., 2004; Zhong et al., 2002) (R.J. Howard and D.L.M., unpublished data). Given the potential for the coil-coiled domain to mediate specific protein-protein interactions, it seemed likely that TRP channel coiled coils might also function as modular assembly domains. To address the importance of coiled coils in TRP channel subunit assembly, we have focused our studies on the cold- and menthol-sensitive channel, TRPM8 (McKemy et al., 2002; Peier et al., 2002). TRPM8 has the shortest C-terminal domain (120 amino acids) of all TRPM subfamily members and contains no other predicted enzymatic motifs or structural elements aside from a predicted coiled-coil domain. These sequence features reduce the likelihood for disrupting other channel-associated activities in the course of targeted deletion studies. Here, we use biochemical methods to show that the last 50 residues of the C-terminal cytoplasmic domain of TRPM8 do, indeed, form a coiled coil that is capable of tetrameric self-assembly. Moreover, we demonstrate that this domain is required for the expression of functional channels at the plasma membrane and is a common feature of TRPM channels.

Results

A Conserved C-Terminal Domain Is Required for TRPM8 Function

Using a coiled-coil prediction algorithm (Lupas et al., 1991), we identified a domain with a high coiled-coil probability at the extreme TRPM8 C terminus (residues 1064–1104). Display of this sequence on a coiled-coil helical wheel diagram shows that the predicted "a" and "d" core positions correspond predominantly to hydrophobic residues. In contrast, the other positions ("b," "c," "e," "f," and "g") are largely polar or charged amino acids (Figure 1A). A similar analysis of other members of the TRPM subfamily indicates that all possess a comparable C-terminal coiled coil at a conserved location in the primary sequence that is 88–120 residues distal to the last putative transmembrane domain, S6 (Figure 1B). We also identified a second potential coiled coil within the N-terminal cytoplasmic domain of TRPM8. Both N- and C-terminal coiled coils are found in TRPM8 orthologs from rat, mouse, chick, and human. However, the N-terminal coil had a much weaker coiled-coil score compared to the C-terminal domain (40% versus 96% probability for the C-terminal coil) and, unlike the C-terminal coil, is not well conserved among other TRPM family members. Thus, we focused our attention on the C-terminal coil.

To investigate the functional significance of the putative C-terminal coiled coil, we expressed a TRPM8 mutant lacking this region (TRPM8Δcc) in *Xenopus* oocytes and examined its sensitivity to thermal and chemical stimuli. Voltage-clamped cells expressing wild-type channels showed robust inward currents to cold (6°C) or menthol (500 μM) (Figure 2A), whereas oocytes injected with TRPM8Δcc cRNA did not respond to either stimulus (Figure 2B). Similar results were obtained with mammalian (HEK293T) cells using calcium imaging to assay for channel function (Figures 2A–2C). Cells were cotransfected with TRPM8 or TRPM8Δcc, plus a TRP channel from a different family (the capsaicin receptor, TRPV1) to control for transfection and calcium imaging. TRPM8- or TRPM8Δcc-expressing cells showed clear differences in menthol responses but no difference in capsaicin sensitivity. TRPV1 and TRPM8 share limited sequence homology (15% identity) and are not known to interact in heterologous systems. Thus, the lack of a response for TRPM8Δcc suggests that the deletion of the coiled coil has rendered the channel nonfunctional.

To control for possible differences in channel expression, we compared TRPM8 levels by Western blotting. These experiments demonstrated that the coiled-coil deletion construct, TRPM8Δcc, was not expressed in either cell type and provide a clear explanation for the lack of functional responses (Figure 2D). The absence of TRPM8Δcc protein indicates that the predicted C-terminal coiled-coil region is required for stable TRPM8 monomer expression.

The Putative Coiled-Coil Region Is Sufficient for Tetrameric Self-Assembly

We asked whether the putative TRPM8 coiled coil could function as an autonomously folded assembly domain.

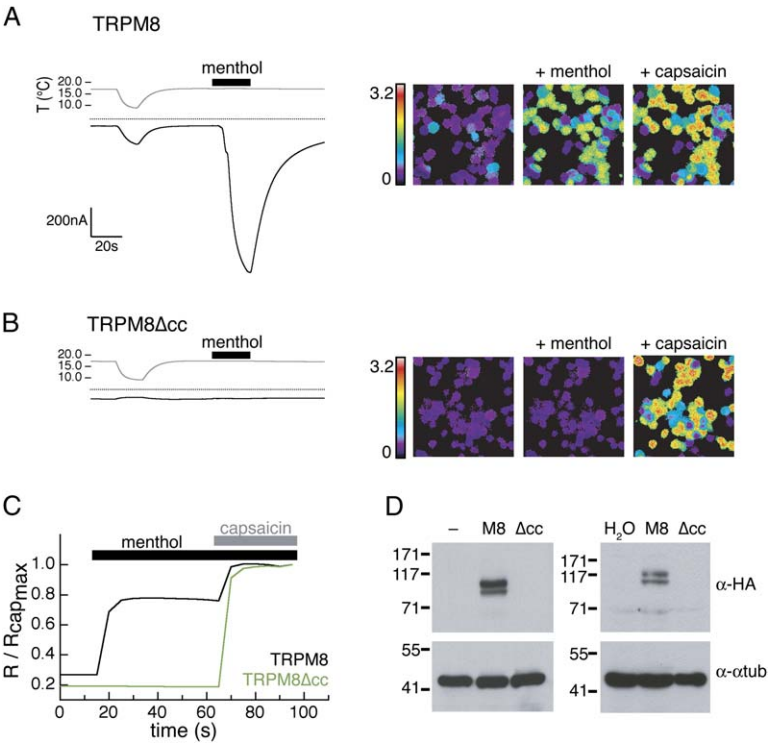

Figure 2. TRPM8 C-Terminal Coiled Coil Is Required for Channel Function and Expression

(A) Oocytes expressing TRPM8 (left) were subjected to a temperature ramp (indicated in gray) and a saturating dose of menthol (500 μM) (indicated by the black bar). Zero-current levels are shown (dashed line). Responses to 500 μM menthol and 1 μM capsaicin in TRPM8/TRPV1-expressing HEK293T cells (right) were measured by fura-2 AM calcium imaging.

(B) Treatments as in (A), for cells expressing TRPM8Δcc (left) and TRPM8Δcc/TRPV1 (right).

(C) Calcium imaging traces normalized to the maximal capsaicin response. Each trace is an average of all capsaicin-responsive cells in the field.

(D) Western blots of the cell lysates of transfected HEK293T cells (left) and injected *Xenopus* oocytes (right). Expected molecular weights for HA-tagged TRPM8 and TRPM8Δcc are 129 kDa and 125 kDa, respectively. Westerns are immunoblotted with an anti-HA (α-HA) or an anti-α-tubulin antibody (α-αtub).

We expressed and purified a fusion protein (termed "HMT," see Experimental Procedures) in which the TRPM8 coiled coil formed the C-terminal domain of a protein that contained, in sequence, His_6, maltose binding protein, and a TEV protease site to make the protein HMT-1055cc. The inclusion of the dual-affinity tags facilitates purification. Purified HMT-1055cc eluted from a gel filtration column with an apparent molecular weight of ~253 kDa. This is significantly larger than the size predicted for a monomer (50.5 kDa) (Table 1) and indicates that the coiled-coil domain self-assembles into a complex of discrete size. Following proteolytic removal of the affinity tags, the purified coiled coil (1055cc) migrated as an ~22 kDa protein in gel filtration (monomer molecular weight, 6.1 kDa), a size that suggests that the coiled-coil domain is a tetramer (Figure 3A).

To test whether the C-terminal coiled coil is a general self-assembly domain for TRPM channels, we examined the self-assembly properties of HMT fusion proteins of the putative coiled coils from TRPM1, TRPM2, TRPM3, TRPM6, and TRPM7 (Figure 1). Gel filtration experiments in which all constructs were assayed at the same monomer concentration (40 μM) demonstrate that all coiled-coil domains tested, except for TRPM1, are capable of some degree of self-assembly (Table 1 and Figure S1 [see the Supplemental Data available online]). Both the TRPM2 and TRPM3 HMT fusions form tetramers. HMT fusions of TRPM6 and TRPM7 run as a mixture of monomers and larger oligomers. Together, these data suggest that the TRPM coiled coil is a general self-assembly domain. The differences in the relative degrees of assembly of the different isolated coiled-coil domains may arise because certain TRPM coils prefer to form heteromeric complexes or because interactions with other parts of the channel may be necessary to stabilize the final folded state.

Table 1. Size Exclusion Chromatography Results for HMT-TRPM Coiled-Coil Fusion Proteins

HMT Fusion	Calculated	Apparent	Stoichiometry	Relative Area
TRPM1	51.0	69.2	1.4	1
TRPM2	50.5	196.3	3.9	1
TRPM3	50.9	195.4	3.8	1
TRPM6	50.7	272.5	5.4	1
		67.5	1.3	5.5
TRPM7	50.8	269.9	5.3	2.7
		64.5	1.3	1
TRPM8	50.5	253.0	5.0	1
HMT	44.5	29.7	0.7	1

Calculated and apparent molecular weights (kDa) are shown.

The relationship between molecular weight and elution volume in gel filtration experiments relies on a correspondence between the hydrodynamic properties of the protein standards and the test protein. Because our experiments were calibrated with globular proteins, the resulting standard curve may not be the most accurate metric for determining the molecular weight of a protein with an elongated structure, such as a coiled coil. Therefore, we used equilibrium sedimentation experiments, which are unsusceptible to the features of protein shape (Laue, 1995), to measure the multimerization state of the purified 1055cc peptide precisely. The equilibrium sedimentation behavior of 1055cc was similar over a range of protein concentrations, rotor speeds, salt concentrations, and detection wavelengths. These data can be described accurately by a single species fit (Figure 3B) and show that the 1055cc complex has a molecular weight four times that of a 1055cc monomer (Table 2). Thus, the putative TRMP8 coiled coil self-assembles into tetramers that mirror the expected stoichiometry of TRP channels.

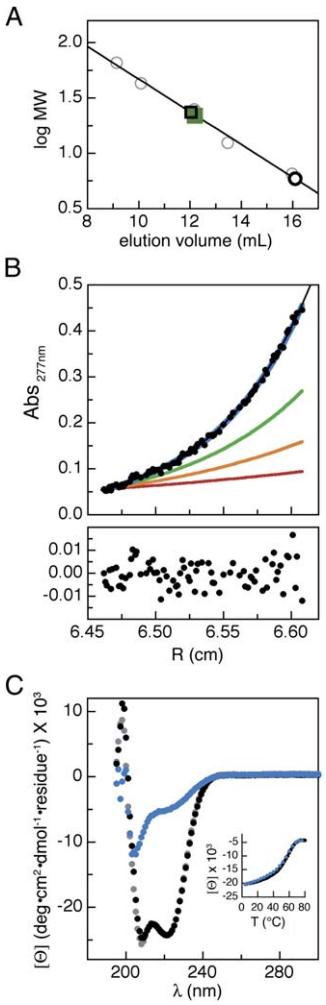

Figure 3. The TRPM8 Coiled-Coil Peptide Forms Tetramers

(A) Gel filtration chromatography data for purified coiled-coil peptide (1055cc) (green squares). Standards (gray circles), predicted monomer (open black circle), and predicted tetramer (open black squares) elution volumes are indicated.

(B) 1055cc peptide analytical ultracentrifugation. Data are shown for 100 μM 1055cc at 27,000 rpm at $Abs_{277\ nm}$. Top panel shows the data (black points), single-species fit (black line), and curves for predicted monomeric (red), dimeric (orange), trimeric (green), and tetrameric (blue) species. Bottom panel shows residual errors of the single-species fit of the data.

(C) Circular dichroism spectra of 100 μM 1055cc peptide at 4°C (black), 80°C (blue), and 4°C post-melt (gray). Inset shows signal at 222 nm during the forward (black) and reverse (blue) temperature scans.

To examine 1055cc's secondary structure, we used circular dichroism (CD) experiments. The 1055cc CD spectrum displays prominent double minima at 208 and 222 nm that are characteristic of an α helix and consistent with formation of a coiled coil (Figure 3C) (Berova et al., 2000). Examination of the CD signal at 222 nm over a range of temperatures (4°C–80°C) showed that the peptide is quite stable (T_m ~60°C). Moreover, the thermal denaturation was reversible (Figure 3C, inset), a feature that is consistent with the ability of this domain to fold autonomously. Together with the equilibrium sedimentation experiments, these data indicate that the C-terminal cytoplasmic domain (residue numbers 1055–1104) is a four-stranded coiled coil.

Table 2. Equilibrium Sedimentation Data for 1055cc

[1055cc] (μM)	Observed Molecular Weight (kDa)	Oligomeric State
50	25.9 ± 1.5	4.2
100	24.9 ± 0.3	4.1
200	23.0 ± 0.3	3.8
Average:	24.6 ± 1.5	4.0

Monomer molecular weight is 6.1 kDa. Errors indicate standard deviations.

A Membrane-Tethered Coiled-Coil Domain Efficiently Inhibits Channel Function and Assembly

The only other well-characterized assembly domain for the voltage-gated ion channel superfamily is the N-terminal T1 domain of Kv potassium channels (Deutsch, 2002). Isolated T1 domains are capable of causing a dominant-negative effect on Kv channel currents when coexpressed with full-length Kv channels (Babila et al., 1994; Li et al., 1992; Shen and Pfaffinger, 1995). As our biochemical experiments demonstrate that the TRPM8 coiled-coil domain folds autonomously, we asked whether it could disrupt TRPM8 function through a dominant-negative mechanism. We measured menthol-evoked currents from *Xenopus* oocytes injected with TRPM8 cRNA and cRNA encoding HMT or HMT-1055cc (TRPM8 residues 1055–1104). We also expressed an HMT coiled-coil fusion that included seven additional N-terminal residues, HMT-1048cc (TRPM8 1048–1104), in the event that a longer coiled-coil construct was more effective at disrupting TRPM8 channel expression. Responses to menthol in both HMT-1055cc- and HMT-1048cc-injected oocytes varied greatly from cell to cell (data not shown). We also found that expression of a coiled-coil construct tagged with the FLAG epitope (Hopp et al., 1988) (FLAG-1048cc) had an insignificant effect on menthol-evoked responses in transfected HEK293T cells as measured by calcium imaging ($p = 0.55$, n = 385–570 cells) (Figure 4A). We reasoned that the inability of HMT- and FLAG-tagged constructs to interfere with TRPM8 activity might be due to a low local concentration of these soluble fusion proteins near the membrane. Consistent with this hypothesis, HEK293T cells transfected with a ten-fold higher ratio of FLAG-1048cc to TRPM8 plasmid DNA showed a slight but significant ($p = 2 \times 10^{-10}$, n = 334–385 cells) decrease in menthol-evoked responses (Figure 4A).

To raise the effective concentration (Jencks, 1987) of 1048cc for TRPM8 channels, we constructed a transmembrane-tethered fusion protein in which the TRPM8 coiled coil was fused C-terminally to the transmembrane domain of CD8 (1048 CD8) (Figure 4B). Coexpression of 1048 CD8 and TRPM8 decreased the average TRPM8 response by 24.5% ± 5.0% (n = 900–1000 cells) and was dose dependent (Figures 4C and 4D).

To evaluate specificity further, cells were also cotransfected with plasmid encoding the capsaicin receptor, TRPV1. Expression of 1048 CD8 had no effect on capsaicin-evoked responses, demonstrating that the dominant-negative action of the TRPM8 coiled coil is

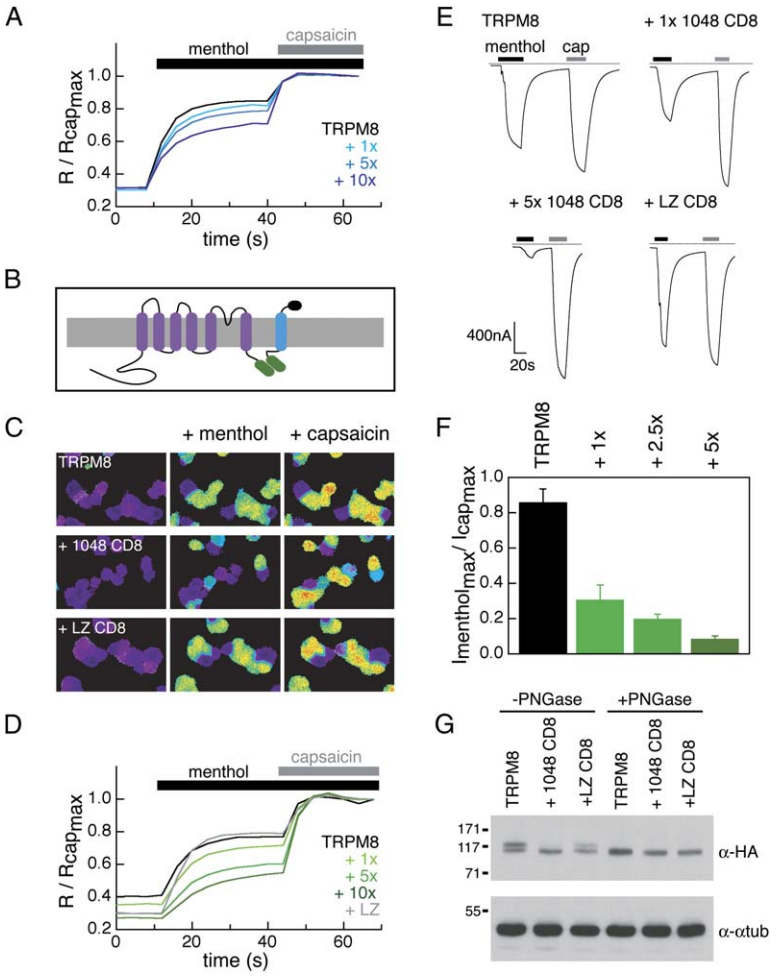

Figure 4. Transmembrane Tethered TRPM8 Coiled Coil Acts as Specific Dominant-Negative Inhibitor of TRPM8 Channel Function

(A) Normalized calcium imaging traces of TRPM8 (black) and TRPM8 + FLAG 1048cc (shades of blue) transfected HEK293T cells. 1×, 5×, and 10× indicate TRPM8:FLAG 1048cc ratios of 1:1, 1:5, and 1:10, respectively (n = 334–570 cells).

(B) Schematic diagram of TRPM8 subunit interaction with the membrane-tethered coiled coil (1048 CD8). TRPM8 coiled coil (green) is C-terminal to the CD8 transmembrane domain (blue). This construct also contains the extracellular domain of the thrombin receptor and a FLAG epitope (black).

(C) Ratiometric calcium imaging of TRPM8, TRPV1, and CD8 coiled-coil constructs (transfected at 5× over TRPM8) in HEK293T cells. Menthol (500 μM) was applied followed by capsaicin (1 μM).

(D) Normalized calcium imaging traces from different ratios of transfected plasmids. +1×, +5×, and +10× represent a 1:1, 1:5, and 1:10 ratio of TRPM8:1048 CD8, respectively. The +LZ trace represents a transfection ratio of 1:5 for TRPM8:LZ CD8. Each trace is the average of 255 to 318 cells.

(E) Representative current traces from injected oocytes with applications of menthol (500 μM) and capsaicin (1 μM). Dashed line indicates zero-current levels. All oocytes were coinjected with TRPM8 and TRPV1 +1048 CD8- and +LZ CD8-injected oocytes also contain the indicated coiled coil. +1× and +5× correspond to 1:1 and 1:5 TRPM8:1048 CD8 cRNA ratios.

(F) Maximal menthol currents normalized to maximal capsaicin currents for increasing ratios of TRPM8:1048 CD8 cRNA (n = 6–9 cells each). Standard errors are shown.

(G) Effects of dominant-negative CD8-anchored coils on TRPM8 glycosylation. Lysates from HA-tagged TRPM8 (TRPM8), HA-tagged TRPM8 and 1048 CD8 (+1048 CD8), and TRPM8 and LZ CD8 (+LZ CD8) transfected HEK293T cells are shown with and without PNGase treatment. Detection with anti-HA (α-HA) and anti-α-tubulin (α-αtub) antibodies are indicated. Molecular weight standards (in kDa) are indicated.

specific for TRPM8 channels. Recent studies have suggested that TRPM8 activation is linked to or influenced by voltage sensitivity of the channel (Brauchi et al., 2004; Voets et al., 2004). While 1048 CD8 alters the magnitude of the menthol-evoked current, the characteristic TRPM8 current-voltage relationship is preserved (Figure S2A). Thus, 1048 CD8 does not alter the biophysical properties of TRPM8.

We also examined the effects of an unrelated coiled coil (GCN4-LI) on TRPM8 responses. This coiled coil forms parallel tetramers (Harbury et al., 1993), and when expressed as a transmembrane fusion (LZ CD8) produced no decrement in menthol-evoked responses ($p = 0.8$, n = 405–555) (Figures 4C and 4D). Similar results were obtained in *Xenopus* oocytes when TRPM8 cRNA was coinjected with TRPV1 and the CD8 fusions (n = 6–9 cells) (Figures 4E and 4F). These data suggest that inhibition of TRPM8 by 1048 CD8 is not due to the presence of a coiled-coil sequence per se, but rather relies on a specific interaction with TRPM8.

Western blots of lysates from TRPM8-transfected HEK293T cells show that the TRPM8 protein runs as two distinct species. Coexpression of 1048 CD8 and TRPM8 caused a preferential decrease in the higher molecular weight species (Figure 4G). Treatment of lysates with PNGase F to remove N-linked glycosylation selectively converted the higher molecular weight species to the lower molecular weight species. These data suggest that the lower band corresponds to unglycosylated TRPM8 and that the inhibitor causes a differential loss of the glycosylated species. Cells coexpressing 1048 CD8 predominantly produced the unglycosylated TRPM8 species, consistent with inhibition of channel assembly at a stage in secretory transport preceding the Golgi (Nagaya and Papazian, 1997); however, some degree of inhibition by 1048 CD8 at the plasma membrane cannot be strictly discounted. In accord with its inability to block functional channel assembly, LZ CD8 had no effect on the glycosylation of TRPM8.

While the loss of glycosylated TRPM8 upon coexpression with 1048 CD8 appears nearly complete by Western blot, we still observe considerable responses to menthol in these cells. Previous studies have reported TRPM8-mediated calcium release from the ER in prostate cancer epithelial cells (Thebault et al., 2005; Zhang and Barritt, 2004). While it is possible that unglycosylated

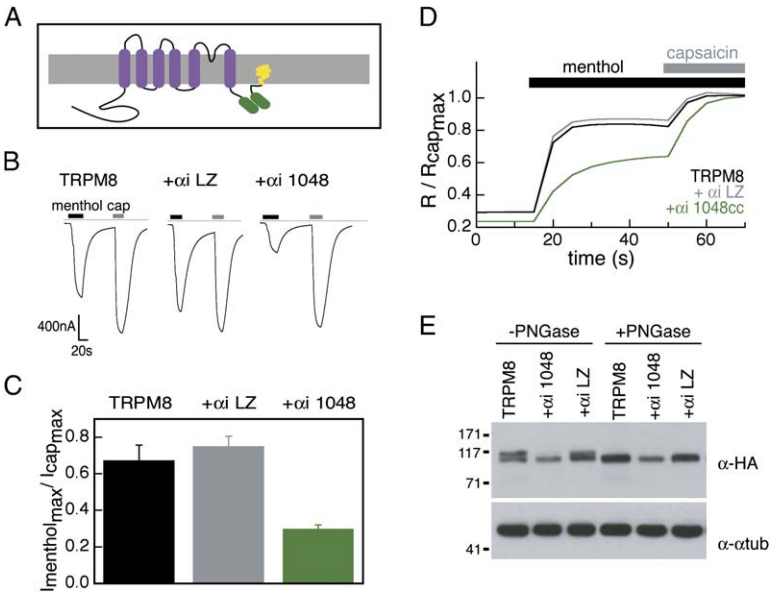

Figure 5. Lipid-Modified Coiled Coil Can Disrupt TRPM8 Channel Function

(A) Schematic diagram of interactions between TRPM8 subunit and the lipid-modified coiled coil (αi 1048). Lipid anchors (yellow) and TRPM8 coiled coil (green) are indicated.

(B) Traces from *Xenopus* oocytes expressing TRPM8, TRPV1, and αi-modified coiled coils. cRNA was injected at a ratio of 1:1:5. Applications of menthol (500 μM) and capsaicin (1 μM) are shown as black and gray bars, respectively. Dashed line indicates zero-current levels.

(C) Average responses from (B), n = 9–13 cells. Maximal menthol-evoked currents were normalized to the maximal capsaicin responses. Error bars indicate standard errors. The p value for the difference between TRPM8 and +αi-1048 is 8.9×10^{-3}.

(D) Normalized calcium imaging traces of TRPM8 (black), TRPM8 + αi-LZ (gray), and TRPM8 + αi-1048 (green) transfected HEK293T cells. Each trace is an average of 1067–1473 cells.

(E) Effects of dominant-negative lipid-anchored coils on TRPM8 glycosylation. Lysates from HA-tagged TRPM8 (TRPM8), HA-tagged TRPM8 + αi 1048 (+αi 1048), and TRPM8 + αi LZ (+αi LZ) transfected HEK293T cells are shown with and without PNGase treatment. Detection with anti-HA (α-HA) and anti-α-tubulin (α-αtub) is indicated. Molecular weight standards (in kDa) are indicated.

TRPM8 is responsible for menthol responses from the ER, we did not observe menthol-evoked calcium store release in TRPM8-transfected HEK293T cells (Figure S2B). Another possibility is that unglycosylated TRPM8 is functional and reaches the plasma membrane, although this is inconsistent with normal mechanisms of protein trafficking, where transmembrane proteins are glycosylated in the Golgi prior to presentation on the plasma membrane (Dempski and Imperiali, 2002; Dunphy and Rothman, 1985). Thus, we conclude that the high sensitivity of calcium imaging detects menthol responses from a small fraction of glycosylated TRPM8 protein on the plasma membrane that is not readily detected by Western blot.

In addition to anchoring the TRPM8 coiled coil to membranes via a transmembrane tether, we also modified FLAG-1048cc with a 15 residue sequence derived from the N terminus of Gαi3 containing myristoylation and palmitoylation sites that target Gαi3 to the plasma membrane (Thiyagarajan et al., 2002) (Figure 5A). Using two-electrode voltage-clamp analysis in oocytes, we found that αi-anchored coiled coils behave identically to the transmembrane-tethered coiled coils. Specifically, coexpression of αi-1048cc with TRPM8 resulted in a substantial decrease (57% ± 6%, n = 9–12 cells) in the average TRPM8 menthol-evoked responses while having no effect on capsaicin-evoked responses in these TRPV1 coinjected cells (Figures 5B and 5C). In contrast, inclusion of a coil of unrelated sequence (αi-LZ) had no effect compared to controls (13% ± 14% increase, n = 7–9 cells) (Figures 5B and 5C). To test whether the dominant-negative effects depended on the particularities of the cell type, we performed similar experiments in transfected HEK293T cells. Averaged responses to menthol were decreased by 31% ± 6% (n = 2327–2595 cells) when αi-1048cc was cotransfected with TRPM8, and addition of αi-LZ did not cause a decrease (4% ± 2% increase, n = 1362–1473 cells) in either TRPM8- or TRPV1-mediated responses (Figure 5D). Western blots showed that coexpression of αi-1048 with TRPM8 resulted in a considerable decrease of the glycosylated TRPM8 species (Figure 5E). This decrease is similar to the effect on TRPM8 glycosylation caused by coexpression of 1048 CD8 (Figure 4G) and suggests that dominant-negative inhibition of TRPM8 by the membrane-tethered coiled coils occurs by similar mechanisms. Thus, the dominant-negative effects appear to arise from the specific action of the TRPM8 coiled-coil assembly domain.

Coiled-Coil Interface Positions Are Required for Channel Function

A key feature of coiled coils is the hydrophobic core formed by the "a" and "d" positions of each strand. To address the importance of these putative core positions in mediating TRPM8 subunit-subunit interactions, we generated alanine point mutations at two "a" and "d" pairs (Figure 6A). Introduction of these mutations into full-length TRPM8 (TRPM8 ccFL and TRPM8 ccLI) resulted in nonfunctional channels, as deduced by lack of menthol responses in transfected HEK293T cells (n = 303–494 cells) (Figure 6B). Gel filtration experiments with purified HMT fusion proteins bearing the same mutations (HMT 1048FL and HMT 1048LI) show that these mutations disrupt the ability of the TRPM8 coiled coils to self-assemble (Figure 6C). Both mutants have apparent molecular weights (68 kDa and 72 kDa, respectively) that are consistent with monomeric species (51.2 kDa

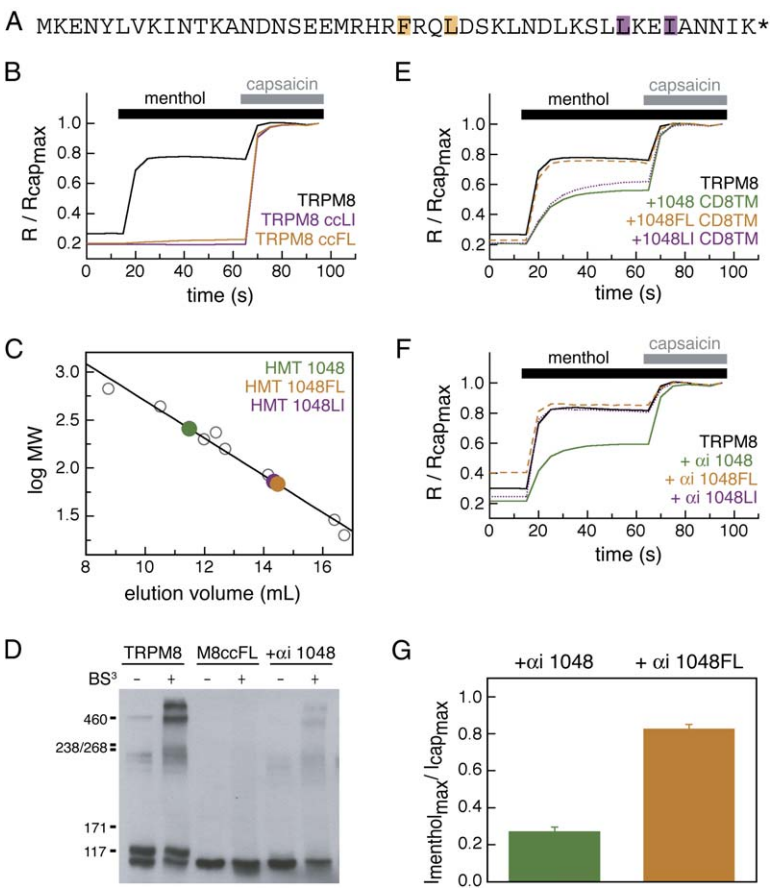

Figure 6. Mutations in TRPM8 Coiled-Coil Core Alter Oligomerization and Channel Function

(A) TRPM8 coiled-coil sequence. Positions of "a" and "d" mutations are indicated, FL→AA (orange) and LI→AA (purple).

(B) Normalized calcium imaging traces from 303 to 494 capsaicin-sensitive cells expressing TRPM8, TRPM8 and TRPM8-ccFL, and TRPM8 and TRPM8-ccLI.

(C) Gel filtration of FL and LI mutant HMT fusion proteins. Wild-type coiled coil (HMT-1048) is shown in green for comparison. HMT-1048FL (orange) and HMT-1048LI (purple) elute as monomers.

(D) BS^3 crosslinking of wild-type TRPM8, full-length TRPM8 bearing the FL coiled-coil mutation (TRPM8ccFL), and TRPM8 coexpressed with αi 1048. No specific crosslinking is seen with TRPM8ccFL. Coexpression of αi 1048 does not prohibit crosslinking of TRPM8.

(E) Normalized calcium imaging traces from HEK293T cells cotransfected with CD8 fusions: 1048 CD8 (green), 1048LI CD8TM (purple), and 1048FL CD8TM (orange). Each trace is an average of 376 to 536 cells.

(F) Normalized calcium imaging traces cells cotransfected with αi fusions, αi-1048 (green), αi-1048FL (orange), and αi-1048LI (purple). Each trace is an average of 398 to 830 cells.

(G) Average maximal menthol responses normalized to maximal capsaicin responses for oocytes expressing TRPM8, TRPV1, and the indicated αi fusions. Standard errors are indicated ($p < 0.001$, n = 9–12 cells).

predicted molecular weights). These results support the idea that the mutations prevent coiled-coil assembly.

In contrast to the effect of deleting the coiled coil (TRPM8Δcc, Figure 2D), impairment (by the FL mutations) in the ability of the coiled coil to associate did not prevent monomer expression as assessed by Western blot, albeit only the unglycosylated form was observed (Figure 6D). Similar results were seen for the TRPM8 ccLI mutant (data not shown). These results suggest that the mutant protein is produced, but retained within the endoplasmic reticulum. This behavior parallels that observed in dominant-negative inhibition by the membrane-tethered coiled coil (Figures 4G and 5E).

To test whether the coiled-coil core mutations disrupt channel function by preventing channel tetramer assembly, we asked whether TRPM8ccFL monomers could be crosslinked to form tetrameric complexes. As a control, lysates from HEK293T cells expressing wild-type TRPM8 channels were treated with an amine-reactive crosslinker, BS^3, yielding complexes that ran as monomer, dimer, tetramer, and higher-order oligomer on SDS-PAGE. In stark contrast, the mutant that disrupts coiled-coil association, TRPM8ccFL, appeared only as a monomer. These data indicate that point mutations in the core of the coiled coil are capable of interfering with self-association of the full-length channel subunits (Figure 6D). We also examined whether suppression of functional channel assembly by coexpression of the αi-1048 dominant-negative coiled coil interfered with the ability to form chemically crosslinked TRPM8 complexes. TRPM8 channels produced under these conditions were predominantly unglycosylated yet retained the ability to form oligomeric species (Figure 6D). This result suggests that TRPM8 subunit assembly occurs prior to the completion of glycosylation events and that glycan addition is a later step in maturation that is likely linked to functional channel expression.

We next asked whether the mutations that disrupt coiled-coil assembly are sufficient to prevent the dominant-negative effect of the isolated coiled coil. 1048FL and 1048LI mutations were expressed in the context of membrane-anchored (αi-1048FL and αi-1048LI) and integral membrane (1048FL CD8 and 1048LI CD8) fusions. αi-1048FL, αi-1048LI, and 1048FL CD8 did not act as dominant-negative inhibitors of the functional expression of TRPM8 in HEK293T cells (n = 398–532 cells) (Figures 6E and 6F). Similarly, αi-1048FL had no effect on menthol-evoked currents in TRPM8-expressing oocytes (n = 9–12 cells) (Figure 6G). Interestingly, 1048LI CD8 did inhibit menthol-evoked responses in TRPM8-expressing HEK293T cells (n = 494–536 cells) (Figure 6E). However, the LI mutations are near the C-terminal end of the coiled coil, suggesting that the CD8 anchor facilitates association of the uninterrupted four remaining turns of the coil that precede these mutations. The position-dependent effects of the FL versus LI mutations further support the notion that the TRMP8 C-terminal coiled coil is part of the full-length channel architecture.

Discussion

All voltage-gated cation channel superfamily pore-forming subunits, with the exception of voltage-gated sodium and calcium channel α subunits, assemble into multimeric complexes to form the ion-conduction pathway (Hille, 2001). For the protein chains to associate following synthesis, the primary sequence must encode determinants that direct subunit assembly and specify whether the subunits form homomeric or heteromeric channel complexes. Despite the generality of this problem, the mechanisms that govern channel assembly are well understood in only one case. Kv channels bear an N-terminal domain, known as T1, that functions as an autonomously folded assembly and specificity domain (Bixby et al., 1999; Kreusch et al., 1998; Li et al., 1992; Shen and Pfaffinger, 1995). Although the T1 domain provides a modular assembly unit that is compatible with the transmembrane architecture shared by voltage-gated ion channel superfamily members, no other channels have T1 domains (Hille, 2001). Distinct domains that are critical for channel assembly and that bear features of coiled-coil motifs (Jenke et al., 2003; Kanki et al., 2004; Zhong et al., 2003) have been identified in the C-terminal cytoplasmic tails of a number of voltage-gated cation channel superfamily members, including KCNQ (Kv7) channels (Schmitt et al., 2000; Schwake et al., 2003), cyclic nucleotide-gated channels (Zhong et al., 2002, 2003), and Eag potassium channels (Jenke et al., 2003; Ludwig et al., 1997). The exact details of how such domains might direct assembly and determine subunit assembly preferences remain unclear.

TRP channels are the largest, most diverse group within the voltage-gated cation channel superfamily (Clapham, 2003). Biochemical and physiological studies suggest that TRP family members form homomeric (Hoenderop et al., 2003; Kedei et al., 2001) or heteromeric complexes depending on the subunit types (Gillo et al., 1996; Hellwig et al., 2005; Schaefer, 2005; Strubing et al., 2001, 2003; Xu et al., 2000). To date, the mechanisms that direct TRP channel assembly and determine the specificity of subunit interactions are not clearly elucidated. TRP channel ankyrin repeats (Erler et al., 2004) and coiled-coil regions (Engelke et al., 2002) have been suggested to play an assembly role; however, evidence supporting any single motif in TRP biogenesis has rested largely on mutational studies that abrogate channel assembly without direct characterization of the relevant biochemical properties of these domains. Our identification and characterization of an autonomously folded C-terminal coiled coil in TRPM8 that functions as an authentic tetramerization domain establishes a mechanism by which TRP channels use coiled coils to direct assembly. Moreover, this domain is conserved among all TRPMs (Figure 1) and shows a conserved biochemical function (Figure S1). The presence of similar domains in other superfamily members suggests that coiled coils are likely to direct channel assembly in other cases and may represent a general assembly strategy.

TRPM8 is thought to function as a homomeric complex. The tetrameric stoichiometry of the coiled-coil motif indicates that, like other superfamily members (Hille, 2001), functional TRPM channels are tetramers. While it is clear that the TRPM8 coiled coil is an assembly domain, we do not yet know whether this domain fosters formation of homomers by excluding interactions with other TRPM subtypes or if additional determinants within the channel sequence are required.

Examination of TRPM coiled-coil sequences shows substantial variability at both the core "a" and "d" positions and the flanking "e" and "g" positions. Studies of designed coiled coils have demonstrated the importance of amino acid identity at "a" and "d" positions for specifying the number of strands in the coil (Harbury et al., 1993), but how natural variation at these positions might affect homomeric or heteromeric preferences among tetramer strands is unknown. The "b," "c," "e," and "g" positions can also make interstrand contacts within the context of a four-stranded coiled coil and may also contribute to assembly specificity (Harbury et al., 1993; Lupas and Gruber, 2005; Woolfson, 2005). Presently, no systematic studies have been done to examine how interactions among these other heptad positions might contribute to specificity in tetramers. It seems plausible that the determinants that encode homotetramer or heterotetramer preferences for a given strand might lie in a combination of central ("a" and "d") and peripheral amino acids ("e," "g," "b," and "c"). The sequence diversity among the TRPM coiled coils may provide an opportunity to address this question.

It is interesting that the majority of putative voltage-gated superfamily channel assembly domains are C-terminal rather than N-terminal. In the Kv channel case, synthesis of the T1 assembly module precedes that of the pore-forming components. Tetramers of nascent channels assemble before the entire polypeptide chain is made and incorporated into the membrane (Deutsch, 2002; Lu et al., 2001; Robinson and Deutsch, 2005; Schulteis et al., 1998). In the case of a C-terminally located assembly domain, the temporal order of assembly must be very different. There is presently little information with regard to how this process might proceed. Modifications of the coiled-coil assembly domain or expression of the dominant-negative assembly module may prove useful for dissecting this question.

Structural studies have shown that ion channel subunits from the voltage-gated ion channel superfamily engage in extensive protein-protein contacts over a large surface area within both the membrane and cytoplasmic domains (Long et al., 2005). Although a single domain may contribute significantly to assembly, it will comprise only a portion of the final total interaction surface between channel monomers. One mechanistic possibility for the utility of distinct assembly domains is that they serve as the critical point of contact that directs specificity and stoichiometry. Once subunits are brought together during early stages of secretory transport, subsequent interactions in the remainder of the complex lead to maturation of the final channel structure. In support of this idea, studies of Kv voltage-gated potassium channel have shown that tetramerization directed by the N-terminal T1 domain is a distinct and early event that occurs in the endoplasmic reticulum before other intersubunit associations are initiated (Nagaya and Papazian, 1997; Schulteis et al., 1998). In the case of very high levels of expression, deletion of T1 does not completely prevent Kv channel formation (Kobertz and

Miller, 1999; Zerangue et al., 2000) and demonstrates that under some conditions other interaction surfaces can support formation of channels, albeit less efficiently.

We found that point mutations in core residues of the TRPM8 coiled coil lead to accumulation of underglycosylated channel protein that is unable to form tetrameric complexes. The block in channel maturation is consistent with a failure to move out of the endoplasmic reticulum and reach the late Golgi (Nagaya and Papazian, 1997). Thus, even though it is the final part of the protein that is made by the ribosome, the coiled-coil domain appears to be required at an early stage of channel maturation. Similar effects of C-terminal coiled-coil deletions have been reported for Eag channels (Jenke et al., 2003). Furthermore, when we attempted to replace the TRPM8 coiled coil with a designed tetrameric coiled coil (GCN4-pLI), we were unable to restore channel function. This result differs from Kv channel protein engineering experiments in which the same designed tetrameric coiled coil could replace (although less efficiently) the role of the T1 domain in promoting channel assembly (Minor et al., 2000; Zerangue et al., 2000). The observation that the TRPM8 coiled coil cannot be replaced with a designed tetrameric coiled coil that should have very similar dimensions and overall architecture suggests that the TRPM8 coiled coil participates in other inter- and intrasubunit interactions that are critical for channel folding and maturation.

Ion channels associate with a range of cellular proteins that act as modulatory factors and that couple channel activity to cellular signaling networks (Hille, 2001). There is increasing evidence that preorganized complexes of the components of such networks form dedicated signaling supramolecular entities (Davare et al., 2001; Hille, 2001). The scaffolding platforms that organize these complexes are just beginning to be defined for channels in the voltage-gated cation channel superfamily. *Drosophila* TRP exists in a large complex at the plasma membrane that includes close association with calmodulin and PLCβ. This complex is organized by the direct binding of the scaffolding protein InaD to TRP via a dedicated PDZ binding domain on the channel (Chevesich et al., 1997; Li and Montell, 2000; Tsunoda and Zuker, 1999). The protein complex that controls β-adrenergic receptor modulation of cardiac I_{KS} channels provides a second example of the importance of supramolecular complexes for channel regulation. Here, the C-terminal coiled-coil domain of KCNQ1 that is also implicated in subunit-subunit assembly (Jenke et al., 2003) interacts with the scaffolding protein yotiao to recruit protein kinase A and protein phosphatase 1 to the channel (Marx et al., 2002). This example suggests that coiled coils may play multiple roles in formation of functional channel complexes. It seems likely that there could be a similar case for TRPM8, where the coiled-coil tetramer could form a site for interaction with other proteins required for regulation of channel activity.

Our data identify an autonomously folded assembly domain that is conserved throughout the TRPM subfamily and appears related to other C-terminal voltage-gated ion channel assembly domains. These results highlight how modular domains are used to solve the problem of directing the assembly of channel pore-forming subunits. The use of a modular assembly is likely to be a common feature of many voltage-gated ion channel superfamily members.

Experimental Procedures

Plasmid Construction

DNA sequences for rat TRPM8 (residues 1055–1104 or 1048–1104) were amplified by PCR and cloned into the NarI/XhoI sites of a pET27(Novagen) derived vector denoted "HMT" (Van Petegem et al., 2004) that contains, in sequence, a His_6-tag, maltose binding protein (MBP), and a cleavage site for the Tobacco Etch Virus protease (TEV) to produce HMT fusion proteins or into BamHI/XhoI sites of pcDNA3-based vectors (Invitrogen) for expression in *Xenopus* oocytes and HEK293T cells. CD8 fusions contain a FLAG epitope and PAR1 thrombin receptor extracellular domain on the N-terminal side of the CD8 transmembrane domain and coiled coils at the C-terminal intracellular side. Lipid modified coiled-coil constructs were made by insertion of oligonucleotides encoding two repeats of amino acids 1–15 of $G_{\alpha}i$. LZ coiled coils were amplified by PCR from a template containing the pIL sequence (Kv1.2_LZ) (Minor et al., 2000). Point mutations were made by Quikchange (Stratagene). The full-length TRPM8 sequence was subcloned into pcDNA3 with a hemaglutinin (HA) epitope tag on the N terminus.

Protein Expression and Purification

HMT fusion proteins were expressed in BL21(DE3) RIL in LB media at 37°C and induced at 0.6–0.8 $OD_{600\ nm}$ with 1 mM IPTG for 3 hr. Cells were harvested by centrifugation (5000 × g, 15 min, 4°C) and frozen. Thawed cells were lysed by sonication in 300 mM NaCl, 10 mM imidazole, and 50 mM $NaPO_4$ (pH 8.0). Insoluble material was removed by centrifugation (12,000 × g, 20 min, 4°C). The resulting soluble fraction was applied to a Ni-NTA column (Qiagen), washed with 300 mM NaCl, 50 mM imidazole, and 50 mM $NaPO_4$ (pH 8.0), and eluted in 300 mM NaCl, 400 mM imidazole, and 50 mM $NaPO_4$ (pH 8.0). Protein was dialyzed in 15,000 MWCO tubing (Spectrapor) against 10 mM NaCl, 20 mM $NaPO_4$ (pH 8.0), followed by purification on a SOURCE Q column (Amersham Biosciences) using a linear gradient to 500 mM NaCl in the same buffer. For purified coiled-coil peptide experiments, protein was dialyzed with His_6-TEV protease (Van Petegem et al., 2004) at room temperature for 2 hr. The reaction was passed over Fast Flow Q resin (Amersham Biosciences) and the flow-through was run over Ni-NTA resin. The column was washed with 300 mM NaCl, 50 mM $NaPO_4$ (pH 8.0) and the coiled coil was purified by elution in 300 mM NaCl, 20 mM imidazole, and 50 mM $NaPO_4$ (pH 8.0). Purified peptide was dialyzed into 100 mM or 200 mM NaCl, 10 mM NaAcetate (pH 5.0).

Size Exclusion Chromatography

Gel filtration with HMT fusion proteins was performed at 4°C using a Superdex 200 HR 10/30 column (Amersham Biosciences) run in 200 mM NaCl, 20 mM Tris (pH 8.0). Purified TRPM8 coiled-coil gel filtration experiments used a Superdex 75 HR 10/30 column run in 200 mM NaCl, 10 mM MES (pH 5.5) at 4°C. Gel filtration calibration standards (Amersham Biosciences) were used to generate standard curves for each column.

Sedimentation Equilibrium Centrifugation

Protein samples in 100 mM or 200 mM NaCl, 10 mM NaAcetate (pH 5.0) were concentrated (3000 MWCO Amicon centrifugal filtration devices, Millipore) and diluted to 200 μM, 100 μM, and 50 μM. Peptide concentration was determined by absorbance (Edelhoch, 1967). Data sets were collected at 4°C in an XL-A ultracentrifuge (Beckman Coulter) at rotor speeds of 15,000, 20,000, and 27,000 rpm. Approach to equilibrium was monitored by absorbance scans at 280 nm every 2 hr until three sequential scans overlapped. Data were fit (ProFit) to the exponential equation describing a single species: $y = \exp(\ln A_0 + ((1 - V\rho)(2\pi\omega)^2)/(2RT)) \times M \times (x^2 - X_0^2))$, where A_0 is the absorbance at X_0, V is the partial specific volume, ρ is the solvent density, ω is the rotor angular velocity, R is the gas constant, T is the sample temperature, M is the calculated molecular mass, and X_0 is the value of the initial x position.

Circular Dichroism

Preparation of peptide sample was the same as for sedimentation equilibrium centrifugation. Wavelength scans from 300 nm to 190 nm were taken using an Aviv Model 215 spectrometer equipped with a peltier device and a 0.1 cm quartz cuvette at 4°C. Thermal denaturation used 2°C step sizes from 4° to 80°C. After a wavelength scan at 80°C, the sample temperature was reduced in 4°C steps to 4°C. Equilibration time at each temperature was 60 s. The T_m (temperature where 50% of the protein is unfolded) was calculated as described (Becktel and Schellman, 1987).

Calcium Imaging

HEK293T cells were transfected with HA-tagged TRPM8, TRPV1, and indicated coiled-coil constructs using Lipofectamine 2000 (Invitrogen). Unless noted otherwise, plasmids were transfected at a mass ratio of 1:0.1:5 of TRPM8:TRPV1:coiled-coil construct, with 0.4 μg TRPM8. These ratios represent 1:0.1:3 molar ratios. One day posttransfection, cells were plated into chambered coverglass coated with poly-D-lysine and incubated at 37°C, 5% CO_2 for 3–5 hr. Cells were loaded with 10 μM fura-2 AM (Molecular Probes), 0.02% pluronic F-127 (Molecular Probes) in a 2 mM Ca^{2+} Ringer's solution (140 mM NaCl, 5 mM KCl, 2 mM $MgCl_2$, 10 mM glucose, 2 mM $CaCl_2$, 10 mM HEPES [pH 7.4]) for 1 hr at room temperature, washed with 2 mM Ca^{2+} Ringer's, and equilibrated in 200 μl of the 2 mM Ca^{2+} Ringer's solution. Agonist application was as follows: 200 μl of 200–500 μM menthol (100–250 μM final) was added at the indicated time point followed by 200 μl of 1 μM capsaicin (0.33 μM final). Ratio data was logged from all capsaicin-sensitive cells in the field, averaged, and normalized to the capsaicin response. Errors indicated are the calculated standard errors.

Deglycosylation and Crosslinking

HEK cells were lysed by trituration in 1% Triton X-100 in PBS and cleared by centrifugation (10,000 × g, 15 min, 4°C). Lysates were treated with PNGase F (New England Biolabs) for 1 hr at 37°C before addition of sample buffer in preparation for SDS-PAGE. Crosslinking was carried out using amine-reactive BS^3 (Pierce). Lysates were prepared as described above, and BS^3 was added to a final concentration of 50 μM. Reactions were incubated at room temperature for 30 min and quenched with 90 mM Tris (pH 7.5) for 15 min before denaturation with SDS-PAGE sample buffer.

Western Blotting

Cell lysates were analyzed by SDS-PAGE using a Mini-PROTEAN II system (Bio-Rad). Gels were transferred to Immobilon-P membranes (Millipore) using a Trans-Blot SD apparatus (Bio-Rad). Blocking and antibody incubations were done in PBS that contained 3% BSA and 0.05% Tween-20 (Sigma). Washing steps used the same solution lacking BSA. Detection of HA-tagged TRPM8, TRPM8Δcc, and TRPM8ccFL used an anti-HA antibody (Covance) and HRP-anti-mouse anitbody (Jackson Immunoresearch). Tubulin controls were blotted with an anti-α-tubulin antibody (Sigma) and the same HRP antibody as above. Blots were visualized with Western Lightning chemiluminescence reagents (PerkinElmer).

Oocyte Recording

After surgical removal and defolliculation by collagenase I (Worthington), *Xenopus* oocytes were maintained at 17°C in ND96 (96 mM NaCl, 2 mM KCl, 1.8 mM $CaCl_2$, 1 mM $MgCl_2$, 5 mM HEPES [pH 7.5]) and injected with cRNA (Mmessage Mmachine kit, Ambion) from HA-tagged TRPM8, TRPV1, and indicated coiled coils. cRNA concentration was determined by absorbance at 260 nm and was injected at a mass ratio of 1:1:5 of HA TRPM8:TRPV1:coiled-coil construct (corresponding to a 1:1:2.5 molar ratio) unless indicated otherwise. Two-electrode voltage-clamp recordings were done at −60 mV in calcium-free ND96 (supplemented with 0.1 mM $BaCl_2$). Agonist solutions were prepared in calcium-free ND96 and perfused into the bath as indicated. Recordings were made with a Geneclamp 500 amplifier (Axon Instruments) controlled by a PC and digitized with a Digidata 1322A (Axon Instruments). Electrodes were filled with 3 M KCl and had resistances of 0.5–1.0 MΩ. Currents were normalized to the maximal capsaicin-evoked responses. Errors shown are calculated standard errors.

Supplemental Data

The Supplemental Data for this article can be found online at http://www.neuron.org/cgi/content/full/51/2/201/DC1/.

Acknowledgments

The authors thank members of the Julius and Minor laboratories for support at all stages of this work. This work was supported by an NSF predoctoral award to P.R.T., awards to D.L.M. from the Alfred P Sloan Foundation, March of Dimes Basil O'Connor Scholar Program, McKnight Foundation for Neuroscience, and grants from the Sandler Family Supporting Foundation and NIH to D.L.M. and D.J. D.L.M. is an Alfred P. Sloan Research Fellow and a McKnight Foundation Scholar.

Received: October 18, 2005
Revised: April 11, 2006
Accepted: June 9, 2006
Published: July 19, 2006

References

Babila, T., Moscucci, A., Wang, H., Weaver, F.E., and Koren, G. (1994). Assembly of mammalian voltage-gated potassium channels: evidence for an important role of the first transmembrane segment. Neuron *12*, 615–626.

Becktel, W.J., and Schellman, J.A. (1987). Protein stability curves. Biopolymers *26*, 1859–1877.

Berova, N., Nakanishi, K., and Woody, R.W. (2000). Circular Dichroism: Principles and Applications, Second Edition (New York: Wiley-VCH).

Bixby, K.A., Nanao, M.H., Shen, N.V., Kreusch, A., Bellamy, H., Pfaffinger, P.J., and Choe, S. (1999). Zn^{2+}-binding and molecular determinants of tetramerization in voltage-gated K^+ channels. Nat. Struct. Biol. *6*, 38–43.

Brauchi, S., Orio, P., and Latorre, R. (2004). Clues to understanding cold sensation: thermodynamics and electrophysiological analysis of the cold receptor TRPM8. Proc. Natl. Acad. Sci. USA *101*, 15494–15499.

Chevesich, J., Kreuz, A.J., and Montell, C. (1997). Requirement for the PDZ domain protein, INAD, for localization of the TRP store-operated channel to a signaling complex. Neuron *18*, 95–105.

Clapham, D.E. (2003). TRP channels as cellular sensors. Nature *426*, 517–524.

Clapham, D.E., Runnels, L.W., and Strubing, C. (2001). The TRP ion channel family. Nat. Rev. Neurosci. *2*, 387–396.

Clapham, D.E., Montell, C., Schultz, G., and Julius, D. (2003). International Union of Pharmacology. XLIII. Compendium of voltage-gated ion channels: transient receptor potential channels. Pharmacol. Rev. *55*, 591–596.

Crick, F.H.C. (1953). The packing of α-helices: Simple coiled-coils. Acta Crystallogr. *6*, 689–697.

Davare, M.A., Avdonin, V., Hall, D.D., Peden, E.M., Burette, A., Weinberg, R.J., Horne, M.C., Hoshi, T., and Hell, J.W. (2001). A beta2 adrenergic receptor signaling complex assembled with the Ca2+ channel Cav1.2. Science *293*, 98–101.

Dempski, R.E., Jr., and Imperiali, B. (2002). Oligosaccharyl transferase: gatekeeper to the secretory pathway. Curr. Opin. Chem. Biol. *6*, 844–850.

Deutsch, C. (2002). Potassium channel ontogeny. Annu. Rev. Physiol. *64*, 19–46.

Dunphy, W.G., and Rothman, J.E. (1985). Compartmental organization of the Golgi stack. Cell *42*, 13–21.

Edelhoch, H. (1967). Spectroscopic determination of tryptophan and tyrosine in proteins. Biochemistry *6*, 1948–1954.

Engelke, M., Friedrich, O., Budde, P., Schafer, C., Niemann, U., Zitt, C., Jungling, E., Rocks, O., Luckhoff, A., and Frey, J. (2002). Structural domains required for channel function of the mouse transient receptor potential protein homologue TRP1beta. FEBS Lett. *523*, 193–199.

Erler, I., Hirnet, D., Wissenbach, U., Flockerzi, V., and Niemeyer, B.A. (2004). Ca2+-selective transient receptor potential V channel architecture and function require a specific ankyrin repeat. J. Biol. Chem. *279*, 34456–34463.

Garcia-Sanz, N., Fernandez-Carvajal, A., Morenilla-Palao, C., Planells-Cases, R., Fajardo-Sanchez, E., Fernandez-Ballester, G., and Ferrer-Montiel, A. (2004). Identification of a tetramerization domain in the C terminus of the vanilloid receptor. J. Neurosci. *24*, 5307–5314.

Gillo, B., Chorna, I., Cohen, H., Cook, B., Manistersky, I., Chorev, M., Arnon, A., Pollock, J.A., Selinger, Z., and Minke, B. (1996). Coexpression of Drosophila TRP and TRP-like proteins in Xenopus oocytes reconstitutes capacitative Ca2+ entry. Proc. Natl. Acad. Sci. USA *93*, 14146–14151.

Harbury, P.B., Zhang, T., Kim, P.S., and Alber, T. (1993). A switch between two-, three-, and four-stranded coiled coils in GCN4 leucine zipper mutants. Science *262*, 1401–1407.

Harbury, P.B., Kim, P.S., and Alber, T. (1994). Crystal structure of an isoleucine-zipper trimer. Nature *371*, 80–83.

Hellwig, N., Albrecht, N., Harteneck, C., Schultz, G., and Schaefer, M. (2005). Homo- and heteromeric assembly of TRPV channel subunits. J. Cell Sci. *118*, 917–928.

Hille, B. (2001). Ion Channels of Excitable Membranes, Third Edition (Sunderland, MA: Sinauer Associates, Inc.).

Hoenderop, J.G., Voets, T., Hoefs, S., Weidema, F., Prenen, J., Nilius, B., and Bindels, R.J. (2003). Homo- and heterotetrameric architecture of the epithelial Ca2+ channels TRPV5 and TRPV6. EMBO J. *22*, 776–785.

Hopp, T.P., Prickett, K.S., Price, V.L., Libby, R.T., March, C.J., Cerretti, P., Urdal, D.L., and Conlon, P.J. (1988). A short polypeptide marker sequence useful for recombinant protein identification and purification. Biotechnology (N. Y.) *6*, 1204–1210.

Howard, J., and Bechstedt, S. (2004). Hypothesis: a helix of ankyrin repeats of the NOMPC-TRP ion channel is the gating spring of mechanoreceptors. Curr. Biol. *14*, R224–R226.

Jencks, W.P. (1987). Catalysis in Chemistry and Enzymology, Dover Edition (New York: Dover Publications).

Jenke, M., Sanchez, A., Monje, F., Stuhmer, W., Weseloh, R.M., and Pardo, L.A. (2003). C-terminal domains implicated in the functional surface expression of potassium channels. EMBO J. *22*, 395–403.

Julius, D., and Basbaum, A.I. (2001). Molecular mechanisms of nociception. Nature *413*, 203–210.

Kanki, H., Kupershmidt, S., Yang, T., Wells, S., and Roden, D.M. (2004). A structural requirement for processing the cardiac K+ channel KCNQ1. J. Biol. Chem. *279*, 33976–33983.

Kedei, N., Szabo, T., Lile, J.D., Treanor, J.J., Olah, Z., Iadarola, M.J., and Blumberg, P.M. (2001). Analysis of the native quaternary structure of vanilloid receptor 1. J. Biol. Chem. *276*, 28613–28619.

Kobertz, W.R., and Miller, C. (1999). K+ channels lacking the 'tetramerization' domain: implications for pore structure. Nat. Struct. Biol. *6*, 1122–1125.

Kreusch, A., Pfaffinger, P.J., Stevens, C.F., and Choe, S. (1998). Crystal structure of the tetramerization domain of the *Shaker* potassium channel. Nature *392*, 945–948.

Laue, T.M. (1995). Sedimentation equilibrium as a thermodynamic tool. Methods Enzymol. *259*, 427–453.

Launay, P., Cheng, H., Srivatsan, S., Penner, R., Fleig, A., and Kinet, J.P. (2004). TRPM4 regulates calcium oscillations after T cell activation. Science *306*, 1374–1377.

Li, H.S., and Montell, C. (2000). TRP and the PDZ protein, INAD, form the core complex required for retention of the signalplex in Drosophila photoreceptor cells. J. Cell Biol. *150*, 1411–1422.

Li, M., Jan, Y.N., and Jan, L.Y. (1992). Specification of subunit assembly by the hydrophillic amino-terminal domain of the *Shaker* potassium channel. Science *257*, 1225–1230.

Liedtke, W., Choe, Y., Marti-Renom, M.A., Bell, A.M., Denis, C.S., Sali, A., Hudspeth, A.J., Friedman, J.M., and Heller, S. (2000). Vanilloid receptor-related osmotically activated channel (VR-OAC), a candidate vertebrate osmoreceptor. Cell *103*, 525–535.

Long, S.B., Campbell, E.B., and Mackinnon, R. (2005). Crystal structure of a mammalian voltage-dependent Shaker family K+ channel. Science *309*, 897–903.

Lu, J., Robinson, J.M., Edwards, D., and Deutsch, C. (2001). T1-T1 interactions occur in ER membranes while nascent Kv peptides are still attached to ribosomes. Biochemistry *40*, 10934–10946.

Ludwig, J., Owen, D., and Pongs, O. (1997). Carboxy-terminal domain mediates assembly of the voltage-gated rat ether-à-go-go potassium channel. EMBO J. *16*, 6337–6345.

Lupas, A.N., and Gruber, M. (2005). The structure of alpha-helical coiled coils. Adv. Protein Chem. *70*, 37–78.

Lupas, A., Van Dyke, M., and Stock, J. (1991). Predicting coiled coils from protein sequences. Science *252*, 1162–1164.

Malashkevich, V.N., Kammerer, R.A., Efimov, V.P., Schulthess, T., and Engel, J. (1996). The crystal structure of a five-stranded coiled coil in COMP: a prototype ion channel? Science *274*, 761–765.

Marx, S.O., Kurokawa, J., Reiken, S., Motoike, H., D'Armiento, J., Marks, A.R., and Kass, R.S. (2002). Requirement of a macromolecular signaling complex for beta adrenergic receptor modulation of the KCNQ1-KCNE1 potassium channel. Science *295*, 496–499.

McKemy, D.D., Neuhausser, W.M., and Julius, D. (2002). Identification of a cold receptor reveals a general role for TRP channels in thermosensation. Nature *416*, 52–58.

Minor, D.L., Jr., Lin, Y.F., Mobley, B.C., Avelar, A., Jan, Y.N., Jan, L.Y., and Berger, J.M. (2000). The polar T1 interface is linked to conformational changes that open the voltage-gated potassium channel. Cell *102*, 657–670.

Montell, C. (2005). The TRP superfamily of cation channels. Sci. STKE *2005*, re3.

Montell, C., Birnbaumer, L., and Flockerzi, V. (2002). The TRP channels, a remarkably functional family. Cell *108*, 595–598.

Nagaya, N., and Papazian, D.M. (1997). Potassium channel alpha and beta subunits assemble in the endoplasmic reticulum. J. Biol. Chem. *272*, 3022–3027.

Peier, A.M., Moqrich, A., Hergarden, A.C., Reeve, A.J., Andersson, D.A., Story, G.M., Earley, T.J., Dragoni, I., McIntyre, P., Bevan, S., and Patapoutian, A. (2002). A TRP channel that senses cold stimuli and menthol. Cell *108*, 705–715.

Robinson, J.M., and Deutsch, C. (2005). Coupled tertiary folding and oligomerization of the T1 domain of Kv channels. Neuron *45*, 223–232.

Rohacs, T., Lopes, C.M., Michailidis, I., and Logothetis, D.E. (2005). PI(4,5)P2 regulates the activation and desensitization of TRPM8 channels through the TRP domain. Nat. Neurosci. *8*, 626–634.

Schaefer, M. (2005). Homo- and heteromeric assembly of TRP channel subunits. Pflugers Arch. *451*, 35–42.

Schmitt, N., Schwarz, M., Peretz, A., Abitbol, A., Attali, B., and Pongs, O. (2000). A recessive C-terminal Jervell and Lange-Nielsen mutation of the KCNQ1 channel impairs subunit assembly. EMBO J. *19*, 332–340.

Schulteis, C.T., Nagaya, N., and Papazian, D.M. (1998). Subunit folding and assembly steps are interspersed during Shaker potassium channel biogenesis. J. Biol. Chem. *273*, 26210–26217.

Schwake, M., Jentsch, T.J., and Friedrich, T. (2003). A carboxy-terminal domain determines the subunit specificity of KCNQ K+ channel assembly. EMBO Rep. *4*, 76–81.

Shen, N.V., and Pfaffinger, P.J. (1995). Molecular recognition and assembly sequences involved in the subfamily-specific assembly of voltage-gated K^+ channel subunit proteins. Neuron *14*, 625–633.

Sotomayor, M., Corey, D.P., and Schulten, K. (2005). In search of the hair-cell gating spring elastic properties of ankyrin and cadherin repeats. Structure *13*, 669–682.

Strubing, C., Krapivinsky, G., Krapivinsky, L., and Clapham, D.E. (2001). TRPC1 and TRPC5 form a novel cation channel in mammalian brain. Neuron *29*, 645–655.

Strubing, C., Krapivinsky, G., Krapivinsky, L., and Clapham, D.E. (2003). Formation of novel TRPC channels by complex subunit interactions in embryonic brain. J. Biol. Chem. *278*, 39014–39019.

Thebault, S., Lemonnier, L., Bidaux, G., Flourakis, M., Bavencoffe, A., Gordienko, D., Roudbaraki, M., Delcourt, P., Panchin, Y., Shuba, Y., et al. (2005). Novel role of cold/menthol-sensitive transient receptor potential melastatine family member 8 (TRPM8) in the activation of store-operated channels in LNCaP human prostate cancer epithelial cells. J. Biol. Chem. *280*, 39423–39435.

Thiyagarajan, M.M., Bigras, E., Van Tol, H.H., Hebert, T.E., Evanko, D.S., and Wedegaertner, P.B. (2002). Activation-induced subcellular redistribution of G alpha(s) is dependent upon its unique N-terminus. Biochemistry *41*, 9470–9484.

Tsunoda, S., and Zuker, C.S. (1999). The organization of INAD-signaling complexes by a multivalent PDZ domain protein in Drosophila photoreceptor cells ensures sensitivity and speed of signaling. Cell Calcium *26*, 165–171.

Van Petegem, F., Clark, K.A., Chatelain, F.C., and Minor, D.L., Jr. (2004). Structure of a complex between a voltage-gated calcium channel beta-subunit and an alpha-subunit domain. Nature *429*, 671–675.

Voets, T., Droogmans, G., Wissenbach, U., Janssens, A., Flockerzi, V., and Nilius, B. (2004). The principle of temperature-dependent gating in cold- and heat-sensitive TRP channels. Nature *430*, 748–754.

Woolfson, D.N. (2005). The design of coiled-coil structures and assemblies. Adv. Protein Chem. *70*, 79–112.

Xu, X.Z., Chien, F., Butler, A., Salkoff, L., and Montell, C. (2000). TRPgamma, a drosophila TRP-related subunit, forms a regulated cation channel with TRPL. Neuron *26*, 647–657.

Zerangue, N., Jan, Y.N., and Jan, L.Y. (2000). An artificial tetramerization domain restores efficient assembly of functional Shaker channels lacking T1. Proc. Natl. Acad. Sci. USA *97*, 3591–3595.

Zhang, L., and Barritt, G.J. (2004). Evidence that TRPM8 is an androgen-dependent Ca2+ channel required for the survival of prostate cancer cells. Cancer Res. *64*, 8365–8373.

Zhong, H., Molday, L.L., Molday, R.S., and Yau, K.W. (2002). The heteromeric cyclic nucleotide-gated channel adopts a 3A:1B stoichiometry. Nature *420*, 193–198.

Zhong, H., Lai, J., and Yau, K.W. (2003). Selective heteromeric assembly of cyclic nucleotide-gated channels. Proc. Natl. Acad. Sci. USA *100*, 5509–5513.